High-field magnetization of $Er(Fe, Ni)_{10}Si_2$ compounds

1999 J. Phys.: Condens. Matter 11 5855

(http://iopscience.iop.org/0953-8984/11/30/314)

J. Phys.: Condens. Matter **11** (1999) 5855–5864. Printed in the UK PII: S0953-8984(99)00530-5

High-field magnetization of $Er(Fe, Ni)_{10}Si_2$ compounds

N Tang†, Z G Zhao‡, E Brück‡, F R de Boer‡, K H J Buschow‡, J L Wang† and F M Yang†

† State Key Laboratory for Magnetism, Institute of Physics, Chinese Academy of Science, Beijing 100080, People's Republic of China
‡ Van der Waals–Zeeman Institute, University of Amsterdam, Valckenierstraat 65, 1018 XE Amsterdam, The Netherlands

Received 31 December 1998, in final form 18 May 1999

Abstract. The structure and magnetic properties of $ErFe_{10-x}Ni_xSi_2$ compounds have been studied. The compounds were found to crystallize in the $ThMn_{12}$-type tetragonal structure for x ranging from 0 to 5. Both lattice parameters, a and c, decrease with increasing Ni content. The Curie temperature reaches a maximum of 566 K at $x = 2$, then decreases strongly for $x > 2$. Alternating-current susceptibility, x-ray diffraction and magnetization measurements show that the easy-magnetization direction of the compounds changes from the easy c-axis at room temperature to the easy cone at low temperature. The rotation process of the Er- and (Fe, Ni)-sublattice magnetization was studied for the compounds with $x > 2$ by means of high-field free-powder magnetization measurements. The contribution of the anisotropy within the basal plane gives rise to oscillations of the high-field magnetization.

1. Introduction

It is well known that binary compounds of the RCo_{12} and RFe_{12} types do not exist, but the 1:12 phase can be stabilized with M as a stabilizing element (M = Ti, V, Cr, Mo, W, Re, Si etc) [1]. These ternary compounds crystallize in the $ThMn_{12}$-type structure (space group $I4/mmm$), which is related to the $CaCu_5$-type hexagonal structure [2]. This is a body-centred-tetragonal structure with one single R site (2a) and three T sites (8f, 8i, 8j).

It has been shown [1] that in these compounds the third element M usually has a strong preference to occupy one of the three crystallographic T sites. The site occupancies in $RT_{12-x}M_x$ compounds have been studied by means of neutron diffraction; the finding was that most M atoms have a strong preference for the 8i site except Si which mainly occupies the 8j and 8f sites [2]. The 8j and 8f sites have larger contact areas with the R site than the 8i site, so a relatively strong influence on the crystal field experienced by the R ion, and possibly also on the R–T interaction, can be expected for Si-containing 1:12 compounds [3].

The indirect exchange interaction between the 3d spins of the T metal and the 4f spins of the R elements in the R–T intermetallic compounds with ferrimagnetic coupling can be studied by measuring the magnetization curves of free powders in high magnetic fields [4]. In $ErFe_{10}Si_2$ compounds, the magnetization of the Fe sublattice is much larger than that of the Er sublattice. In order to investigate the R–T exchange interaction in this type of compound, it is useful to substitute non-magnetic elements for Fe, so as to decrease the critical field for the rotation process. Nickel is the best choice because in R–T compounds Ni is often non-magnetic, although its magnetization cannot be neglected completely. In the present paper,

0953-8984/99/305855+10$30.00

the effects of Ni on the magnetic properties of the $ThMn_{12}$-type $ErFe_{10-x}Ni_xSi_2$ compounds are presented.

2. Experiment

Quasi-ternary $ErFe_{10-x}Ni_xSi_2$ compounds, with $x = 0.0$, 1.0, 2.0, 3.0, 3.5, 4.0, 4.5 and 5.0, were prepared by arc melting the constituent elements under purified argon. The ingots were wrapped in Ta foil and annealed in a quartz tube filled with purified argon at 1050 °C for three weeks. The annealed samples were water quenched. X-ray diffraction (XRD) showed that all of the compounds with $x \leqslant 6$ crystallize in the tetragonal $ThMn_{12}$ structure except for small amounts of impurity phases. Although some of the ternary Ni compounds, like $YNi_{10}Si_2$ [5], $GdNi_{10}Si_2$, $DyNi_{10}Si_2$ and $HoNi_{10}Si_2$ [6], can be synthesized, it was difficult to prepare single-phase $ErFe_{10-x}Ni_xSi_2$ samples for $x > 6$.

The ac susceptibility was measured for bulk samples in the temperature range 4.2–300 K with an ac current of 10 mA at a frequency of 100 Hz. Thermal magnetic analysis (TMA) was performed by using a vibrating-sample magnetometer (VSM) from room temperature to 850 °C in a field of 0.04 T. The magnetic isotherms at 4.2 K of all compounds were measured in the high-field installation at the University of Amsterdam [7] in fields up to 38 T. The samples consisted of finely powdered particles (<40 μm), which were free to rotate into their minimum-energy direction during the measurements.

3. Results

The lattice parameters a, c, derived from x-ray diffraction patterns, are listed in table 1, together with the magnetic properties of the $ErFe_{10-x}Ni_xSi_2$ compounds studied. Both a and c decrease with increasing the Ni content x.

Table 1. Lattice constants a, c and some magnetic parameters of $ErFe_{10-x}Ni_xSi_2$ compounds. T_C represents the Curie temperature, T_{sr} the spin-reorientation temperature, $M(0)$ the spontaneous moment and M_{Fe-Ni} the moment of the transition-metal (Fe–Ni) sublattice, obtained by adding the Er-sublattice moment of 9 μ_B to $M(0)$.

x	a (Å)	c (Å)	T_C (K)	T_{sr} (K)	$M(0)$ (μ_B/f.u.)	M_{Fe-Ni} (μ_B/f.u.)
0.0	8.3884	4.7480	538	18	10.0	19.0
1.0	8.3880	4.7378	561	22	12.0	21.0
2.0	8.3753	4.7187	566	29	7.8	16.8
3.0	8.3682	4.7137	556	47	6.2	15.2
3.5	8.3592	4.7030	549	63	5.3	14.3
4.0	8.3444	4.6918	530	88	4.6	13.6
4.5	8.3421	4.6920	513	103	3.9	12.9

The Curie temperatures of the $ErFe_{10-x}Ni_xSi_2$ compounds, derived from the thermomagnetic curves $M(T)$ measured above room temperature, are shown in figure 1. The temperature dependence of the ac susceptibility is shown in figure 2. For all compounds, the ac susceptibility shows an indication of a spin reorientation. As illustrated in figure 1, the spin-reorientation temperature T_{sr} increases very strongly with increasing Ni content.

In order to obtain information regarding the easy-magnetization direction (EMD) at room temperature, XRD measurements on magnetically aligned samples of $ErFe_9NiSi_2$ and $ErFe_{6.5}Ni_{3.5}Si_2$ were performed. The results obtained are shown in figures 3 and 4, where they

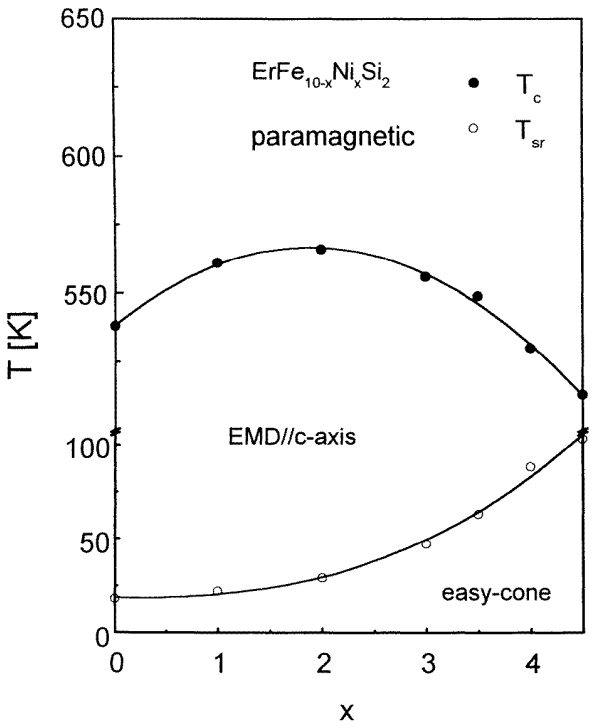

Figure 1. The spin phase diagram of $ErFe_{10-x}Ni_xSi_2$ compounds. The solid curves are guides to the eye.

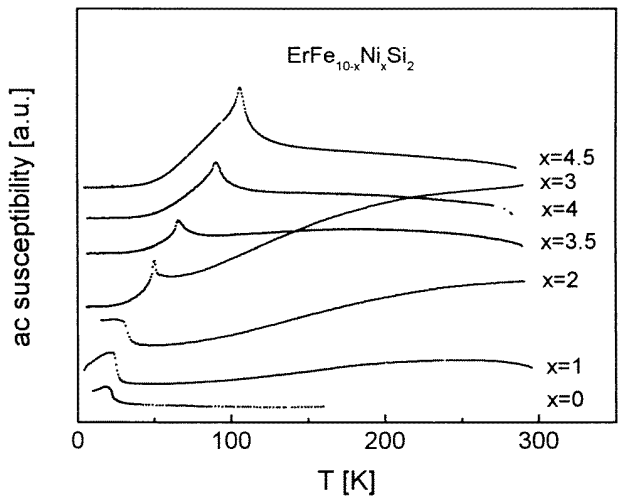

Figure 2. The temperature dependence of the ac susceptibility of $ErFe_{10-x}Ni_xSi_2$ compounds in the temperature range from 4.2 to 300 K, measured in an ac field of 1.2 mT with a frequency of 100 Hz.

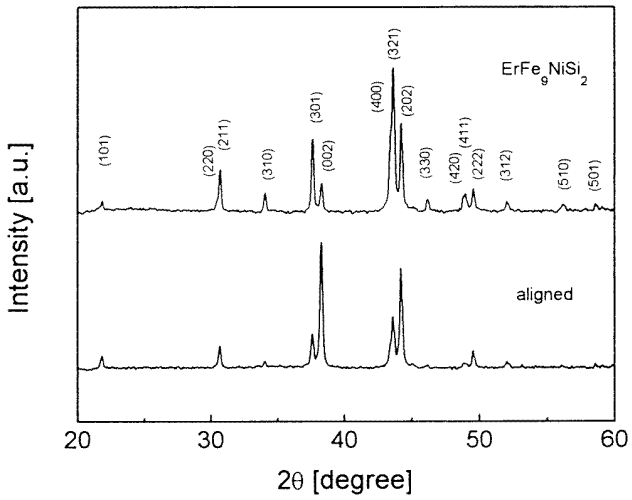

Figure 3. X-ray diffraction patterns of randomly oriented (top) and magnetically aligned (bottom) powder samples of $ErFe_9NiSi_2$.

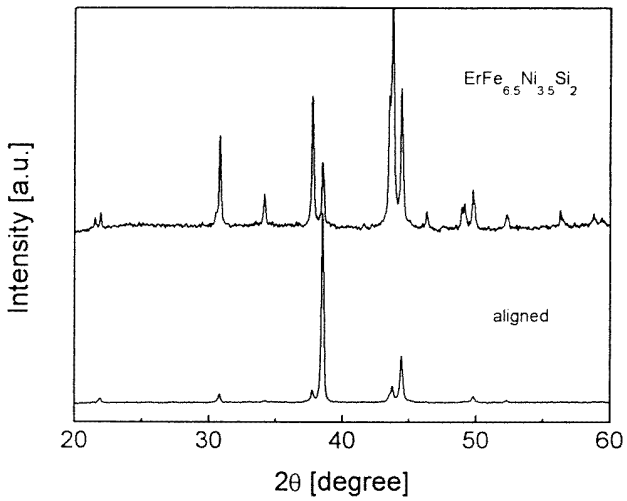

Figure 4. X-ray diffraction patterns of randomly oriented (top) and magnetically aligned (bottom) powder samples of $ErFe_{6.5}Ni_{3.5}Si_2$.

are compared with the results obtained on randomly oriented powder. The EMD below room temperature was also studied by measuring the magnetization of magnetically aligned samples at various temperatures in an applied field of 1 T as a function of the angle between the applied field and the alignment direction. As examples, figures 5 and 6 show the measured results for $ErFe_9NiSi_2$ and $ErFe_{6.5}Ni_{3.5}Si_2$, respectively.

High-field magnetization measurements have been performed at 4.2 K on free powder particles of the $ErFe_{10-x}Ni_xSi_2$ compounds (figure 7) with the purpose of studying the Er-

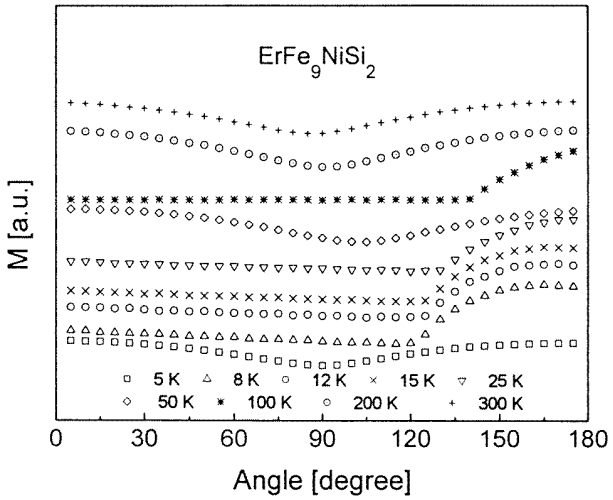

Figure 5. The dependence of the magnetization of $ErFe_9NiSi_2$ on the angle between the alignment direction (the easy axis at room temperature) and the direction of the applied field (1 T).

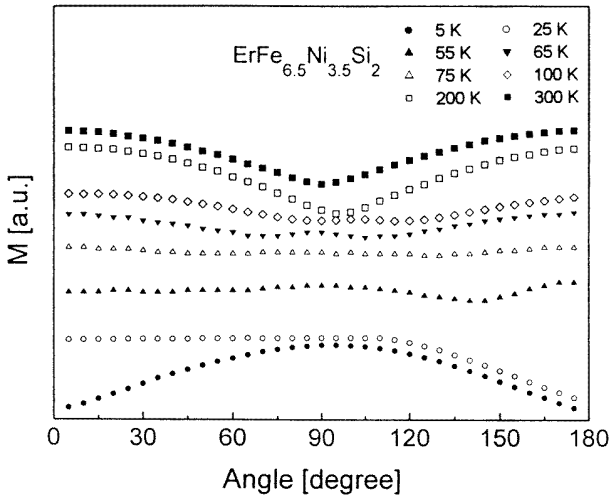

Figure 6. The dependence of the magnetization of $ErFe_{6.5}Ni_{3.5}Si_2$ on the angle between the alignment direction (the easy axis at room temperature) and the direction of the applied field (1 T).

(Fe, Ni) exchange interaction in these compounds. The measurements were performed in quasi-stationary fields up to 35 T and in fields decreasing continuously from 38 T. The low-field part of the magnetization curves in figure 7 was used to obtain values for the spontaneous magnetization $M(0)$, by extrapolation of the magnetization to zero field. It can be seen from table 1 that $M(0)$ first increases, from 10.0 μ_B/f.u. for $x = 0$ to 12.0 μ_B/f.u. for $x = 1$, then decreases from 12.0 μ_B/f.u. for $x = 1$ to 3.9 μ_B/f.u. for $x = 4.5$.

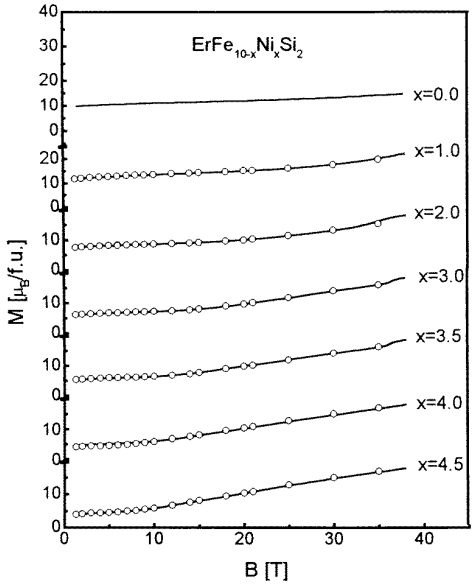

Figure 7. Free-powder magnetization curves at 4.2 K of $ErFe_{10-x}Ni_xSi_2$ compounds. The circles represent the measurements in quasi-stationary fields and the lines correspond to the measurements in fields decreasing linearly with time at a rate of 50 T s^{-1}.

4. Discussion

The dependence of T_C on the Ni content is shown in figure 1. The Curie temperature increases first and reaches a maximum of 566 K at $x = 2$, then decreases strongly for $x > 2$. This behaviour is very similar to that of $HoFe_{10-x}Ni_xSi_2$ compounds [8], but different from that of $YCo_{10-x}Ni_xSi_2$ compounds [5] for which the Curie temperature decreases monotonically with increasing Ni content. The concentration dependence of T_C mentioned above is probably due to changes of the Ni and Fe moments associated with a change of the band structure.

It can be seen from the XRD diagrams presented in figures 3 and 4 that for magnetically aligned samples, the intensity of the (002) reflection has considerably increased compared to that of the randomly oriented powder. This indicates that the easy-magnetization direction is in these two samples along the *c*-axis. In figures 3 and 4, the basal-plane reflections in the XRD patterns of the magnetically aligned samples have not disappeared completely, which may be associated with some misalignment of the powder particles.

From the magnetization measurement results for $ErFe_9NiSi_2$ shown in figure 5, it is not possible to see how the EMD changes from 5 K to room temperature. Very probably, this is due to incomplete alignment of the sample. However, for $ErFe_{6.5}Ni_{3.5}Si_2$ (figure 6) the situation is much clearer. At low temperatures, the EMD is very probably in the *ab*-plane. As temperature increases, two minima occur in the angle dependence of M, which indicates that the EMD changes from the easy plane to an intermediate direction. With increasing temperature, the EMD angle changes from 90°, corresponding to an easy *ab*-plane, to 0°, corresponding to an easy *c*-axis.

Our result for $x = 0$ is in agreement with the data reported by Li *et al* [9]. The EMD of $YFe_{10}Si_2$ is along the *c*-axis at all temperatures and in $ErFe_{10}Si_2$ the EMD changes from an

intermediate direction at low temperatures to the c-axis at higher temperature. This supports our view that, in the $ErFe_{10-x}Ni_xSi_2$ compounds, the EMD above the spin-reorientation temperature should be along the c-axis, whereas below the spin-reorientation temperature the anisotropy should be minimum for an intermediate direction.

These findings can be understood in terms of the magnetocrystalline anisotropy of the Er and Fe sublattices. From crystalline-electric-field (CEF) calculations [1], the sixth-order CEF term should be dominant at low temperature which leads to an EMD tilt with respect to the c-axis. At higher temperatures, the sixth-order CEF term has decreased strongly. The (Fe, Ni)-sublattice anisotropy dominates, which gives rise to the occurrence of a spin reorientation in the intermediate-temperature regime. Introduction of Ni decreases the Fe-sublattice anisotropy and, for a constant anisotropy of the Er sublattice, one expects T_{sr} to increase with increasing Ni content. This result also shows that at low temperatures the anisotropy constant K_1 ($=K_1^{Er} + K_1^{T}$) is negative in all $ErFe_{10-x}Ni_xSi_2$ compounds [10]. The basal-plane anisotropy plays an important role in the magnetization process, as will be shown for the high-field magnetization curves described below.

The results of free-powder magnetization measurements (figure 7) show that after an initial increase, the values for the spontaneous magnetization $M(0)$ decrease with increasing Ni content. $M(0)$ shows a maximum at around 10% Ni (see table 1); this phenomenon is reminiscent of the magnetic properties of Fe–Ni alloys, for which there is also a maximum of the magnetization [11]. As the Fe and Ni atoms surround each other, the local density of 3d-electron states of Fe atoms changes upon introduction of Ni atoms. In other words, the number of spin-up and spin-down electrons will become affected by the introduction of Ni. As a result, the moment of Fe may decrease whereas that of Ni may increase and the total magnetization may become larger or smaller than that of the parent alloy or compound.

The first critical field [12], where the rotation of the R and 3d moments towards each other starts, also decreases with increasing Ni content. It can be seen in figure 7 that, on increasing the Ni content, the rotation process gradually enters the accessible field range, becoming clearly observable for $x \geqslant 3$. For the compounds with $x = 2.0$, 3.0, 3.5, 4.0 and 4.5, it has been found that, above the first critical field, the magnetization varies either in a discontinuous way or in an oscillatory way. Figure 8 shows $\mathrm{d}M/\mathrm{d}B$ versus B for the compounds with $x = 2.0$, 3.0 and 3.5. It is clear that in the magnetization of the compounds with $x > 2$, a jump occurs at around 35 T. With the compounds with $x = 3.0$ and 3.5, some small oscillations are also observed. This complex behaviour may be attributed to the presence of considerable magnetic anisotropy of both the Er and the (Fe, Ni) sublattice in the ab-plane (which will be discussed below). In this case, the high-field free-powder magnetization will deviate from the simple linear $B/M = n_{RT}$ behaviour.

On the basis of a molecular-field description, the total energy E for a ferrimagnetic RT compound free-powder sample can be written as

$$E = E_{an}^{R} + E_{an}^{T} + n_{RT} M_R M_T \cos\alpha - MB$$

where E_{an}^{R}, E_{an}^{T}, M_R and M_T represent the anisotropy energies and the magnetic moments of the R and T sublattices. α is the angle between the two sublattice moments and B is the applied field. M is the total magnetization of the compound:

$$M = \sqrt{M_R^2 + M_T^2 + 2M_R M_T \cos\alpha}.$$

For a tetragonal structure,

$$E_{an} = K_1 \sin^2\theta + K_2 \sin^4\theta + K_3 \sin^6\theta + K_4 \sin^4\theta \cos 4\varphi$$

where θ is the angle between the tetragonal axis and the magnetization and φ is the angle between the component of the magnetization in the basal plane and the [100] axis.

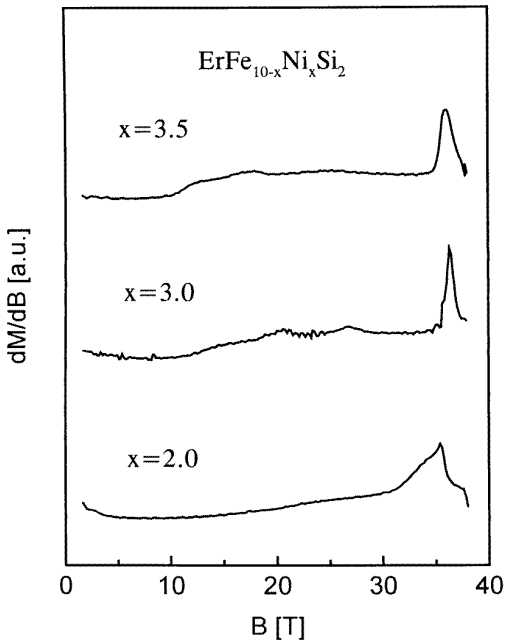

Figure 8. The field dependence of $\mathrm{d}M/\mathrm{d}B$ for $ErFe_{10-x}Ni_xSi_2$ compounds with $x = 2.0$, 3.0 and 3.5.

The equilibrium directions of M_R and M_T can be determined by minimizing the free energy E with respect to θ_R, θ_T and $\varphi_R - \varphi_T$ [13]. For a free-powder sample, three simple solutions may be obtained when M changes from $|M_R - M_T|$ to $M_R + M_T$:

(a) The magnetocrystalline anisotropy of the transition-metal sublattice is zero; $E_{an}^T = 0$ [4]:

$$\frac{B}{M} = n_{RT}.$$

The magnetization depends linearly on the field with a slope $1/n_{RT}$.

(b) The R sublattice and the T sublattice both have uniaxial anisotropy and only K_1 is taken into account [12]:

$$\frac{B}{M} = n_{RT} - \frac{2K_1^R K_1^T}{M_R M_T |K|}\cos\alpha$$

with $|K| = [(K_1^R)^2 + (K_1^T)^2 + 2\ K_1^R K_1^T \cos 2\alpha]^{1/2}$. The magnetization deviates from the simple linear behaviour.

(c) The R sublattice and the T sublattice both have easy-plane anisotropy and there is non-zero anisotropy within the basal plane. For the tetragonal structure [13],

$$\frac{B}{M} = n_{RT} - \frac{16K_4^R K_4^T}{M_R M_T |K|}\cos\alpha\cos 2\alpha$$

with $|K| = [(K_4^R)^2 + (K_4^T)^2 + 2K_4^R K_4^T \cos 4\alpha]^{1/2}$.

The magnetization curve will cross the straight line $B/M = n_{RT}$ three times at $\alpha_1 = \pi/4$, $\alpha_2 = \pi/2$ and $\alpha_3 = 3\pi/4$.

According to the above discussion, the easy-axis anisotropy of the Fe sublattice and the intermediate direction of the Er sublattice result in the total magnetization of $ErFe_{10-x}Ni_xSi_2$ compounds at 4.2 K to deviate along the intermediate direction. In this case, we cannot use the formulae to explain the high-field magnetization process exactly. However, the oscillations in the magnetization curves can be considered as an indication that the anisotropy within the basal plane should be taken into account. If we use a simple model in which only the anisotropy constant K_4 of the two sublattices contributes to the free energy of the single-crystalline particle, the influence of K_4 on the total magnetic moment M can be calculated and the result is plotted in figure 9. When M changes from $|M_R - M_T|$ to $M_R + M_T$, for a non-zero value of K_4^R, there will be no oscillations when K_4^T is zero. Four oscillations are expected to appear around the linear $B/M = n_{RT}$ curve when K_4^T becomes comparatively large. Although there are some indications of oscillations in the high-field magnetization curves of the $ErFe_{10-x}Ni_xSi_2$ compounds with compositions between $x = 2.0$ and 4.5, these oscillations are too small to be analysed in detail. Single crystals are necessary for studying such oscillations along the main crystallographic directions.

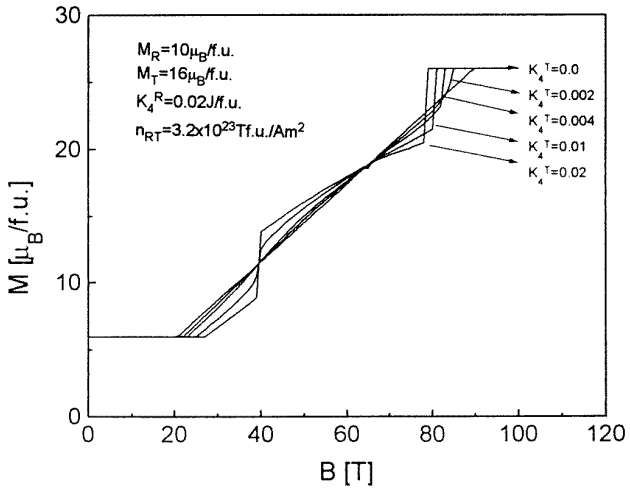

Figure 9. The influence on the magnetic moment M of the magnetic anisotropy constants K_4^R and K_4^T of the R and T sublattice, respectively. K_4^T and K_4^R are both expressed in J/f.u.

References

[1] Li Hong-shuo and Coey J M D 1991 *Handbook of Magnetic Materials* vol 6, ed K H J Buschow (Amsterdam: North-Holland) p 1
[2] Johnson Q and Smith G S 1968 *Lawrence Radiation Laboratory Report* UCRL-71094
[3] de Mooij D B and Buschow K H J 1987 *Philips J. Res.* **42** 246
[4] Verhoef R, de Boer F R, Franse J J M, Denissen C J M, Jacobs T H and Buschow K H J 1989 *J. Magn. Magn. Mater.* **80** 41
[5] Tang H, Zhang D, Brück E, de Boer F R and Buschow K H J 1997 *Physica* B **240** 104
[6] Li Q A, Tang N, de Boer F R and Buschow K H J 1993 unpublished
[7] Gersdorf R, de Boer F R, Wolfrat J C, Muller F A and Roeland L W 1983 *High Field Magnetism* ed M Date (Amsterdam: North-Holland) p 277
[8] Tang H, Brück E, de Boer F R and Buschow K H J 1996 *J. Alloys Compounds* **243** 85

[9] Li Qingan, Lu Yi, Zhao Ruwen, Tegus O and Yang Fuming 1991 *J. Appl. Phys.* **70** 6116
[10] Asti G and Bolzoni F 1980 *J. Magn. Magn. Mater.* **20** 29
[11] Bozorth R M 1951 *Ferromagnetism* (New York: Van Nostrand)
[12] Zhao Z G, Li X, Brabers J H V J, de Châtel P F, de Boer F R and Buschow K H J 1993 *J. Magn. Magn. Mater.* **123** 74
[13] Zhao Z G, Tang N, de Boer F R, de Châtel P F and Buschow K H J 1994 *Physica* B **193** 45